4-12-2021

Road network detection based on improved FLICM-MRF method using high resolution SAR images

Lamei Zhang

Chenwei Jiang

Bin Zou

Zhijun Qiao
The University of Texas Rio Grande Valley, zhijun.qiao@utrgv.edu

Recommended Citation

Lamei Zhang, Chenwei Jiang, Bin Zou, and Zhijun Qiao "Road network detection based on improved FLICM-MRF method using high resolution SAR images", Proc. SPIE 11730, Big Data III: Learning, Analytics, and Applications, 117300H (12 April 2021); https://doi.org/10.1117/12.2587444

Road network detection based on improved FLICM-MRF method using high resolution SAR images

Zhang, Lamei, Jiang, Chenwei, Zou, Bin, Qiao, Zhijun

Lamei Zhang, Chenwei Jiang, Bin Zou, Zhijun Qiao, "Road network detection based on improved FLICM-MRF method using high resolution SAR images," Proc. SPIE 11730, Big Data III: Learning, Analytics, and Applications, 117300H (12 April 2021); doi: 10.1117/12.2587444

SPIE.

Event: SPIE Defense + Commercial Sensing, 2021, Online Only

Road Network Detection based on Improved FLICM-MRF Method using High Resolution SAR Images

Lamei Zhang[1], Chenwei Jiang[1], BinZou[1], Zhijun Qiao[2]
[1]Department of information Engineering, Harbin Institute of Technology, Harbin, China
[2]School of Mathematical & Statistical Sciences-MAGC, University of Texas–Rio Grande Valley, TX, USA

ABSTRACT

The automatic detection of road network from satellite and aerial images is highly significant in many actual applications, for instance, urban traffic measurement, military emergency response, and vehicle target tracking. Compared with other high-resolution satellite remote sensing images, high-resolution synthetic aperture radar (SAR) has become a popular research perspective for road detection owing to its insensitivity to the atmosphere and sun-illumination. However, the method of road network detection is still lagging due to the strong multiplicative speckle noise and complex background interference, causing the loss and break in the road segment extraction results. Aiming to solve this problem, a three-step road network detection framework is proposed. In the first step, the road segment candidates are extracted by the Fuzzy Local Information C-Means (FLICM) algorithm based on the gray-level co-occurrence matrix(GLCM) with Markov Random Fields (MRF), and it contains an adaptive parameter selection procedure which is presented for adjusting joint clustering parameters. In order to reduce false segments, we perform the local processing which combines the morphological operation, linearity index, and local Hough transform in the second step. Finally, as for the global road segment connection, we propose an improved region growing algorithm which fully considering the rationality of road elements to gain the road network. Compared with the traditional region growing algorithm, the proposed method can effectively promote the improvement of the integrity of the road network detection. Moreover, the performance of the proposed method is evaluated by comparing the results with the ground truth road map and the evaluation index including the completeness, correctness, and quality factor. In experiments, the algorithm has been verified with the SAR images from the different resolutions of the GF-3 satellite SAR image. The results of the various real images demonstrate that the proposed algorithm has improved considerably the adaptability and efficiency of road detection compared with other methods.

Keywords: synthetic aperture radar, FLICM-MRF, road network detection

1. INTRODUCTION

Synthetic Aperture Radar(SAR) is widely used in environmental monitoring and modern urbanization construction owing to all-weather and all-time imaging capabilities and widespread coverage [1]. Thus, the need for detection of SAR has become urgent and important. And detection of roads based on SAR images has been employed in many practical applications, e.g., urban traffic measurement, military emergency response, and navigation [2]-[3]. However, road detection is still scientifically challenging while accurate and effective methods are yet to be developed. Therefore, it is essential to study the algorithm of road network detection of SAR images.

The road extraction processing can be classified into two main categories: semiautomatic and automatic extraction. The former usually requires human interaction to obtain the road segment seeds, while the latter determines the seeds by utilizing the features. To fully make use of the function of image processing ability of a computer, while at the same time, reduce the abundant time cost, the automatic road network detection of SAR is gradually becoming a popular research direction.

In the last two decades, to cope with the automatic road detection task, many road network extraction algorithms for SAR images have been proposed, which mostly include three-level processing. In the low-level processing, the road segment candidates are extracted by edge detectors, line detectors, and fuzzy clustering algorithms [4]-[7]. For example, Roger Fjørtoft[4] has proposed the radio of exponentially weighted averages (ROEWA) operator that proved to be an

Big Data III: Learning, Analytics, and Applications, edited by Fauzia Ahmad, Panos P. Markopoulos, Bing Ouyang, Proc. of SPIE Vol. 11730, 117300H

efficient multi- -edge detector for SAR image. Tupin et al. [5] proposed an unsupervised detection algorithm that utilize local line detectors to detect the edge information of the road. FCM is one of the most widely used fuzzy clustering algorithms in image segmentation, while it is sensitive to noise [6]. To address this problem, Krinidis and Chatzis [7] proposed a robust fuzzy local information C-means (FLICM) algorithm, which considers the local spatial information by increasing a fuzzy factor into the objective function. The aim of medium-level processing is to select the qualified road elements from the redundant extracted road segment candidates that use the combination of the geometric and spatial local operations, including linearity index, morphological operation, Bayesian analysis, and local Hough transform [8]-[11]. Due to the impact of strong multiplicative speckle noise and complex background interference, there is some loss and break in the output of the lower-level steps which leads to the high-level road network reconstruction processing. In order to fill the gaps between the nearby road elements, the processing takes the spatial relationships and grayscale change into consideration, which utilizing the methods includes genetic algorithm(GA)[12], Markov random fields (MRF)[13]-[14], and region growing(RG)[15]-[16].

In this paper, a three-level road network detection framework is proposed. First, the road segment candidates are extracted by a weighted local information FLICM-MRF algorithm with pixel intensity and texture feature. Second, the qualified road elements are obtained from the local operations based on the road geometric and spatial features. Finally, as for the connection processing, an improved RG algorithm with the rationality of road network reconstruction is proposed to build the whole road network information, which performs better than the traditional algorithm.

2. METHODOLOGY

In this section, the methodology adopted in this work is introduced in detail, explaining the principle and implementation steps: 1) road features extraction procedure to obtain road candidate elements; 2) false road element removal procedure to select the eligible road segment; 3) road elements linking procedure to complete the global reconstruction. The framework for the SAR image road network detection procedure is described in Figure1.

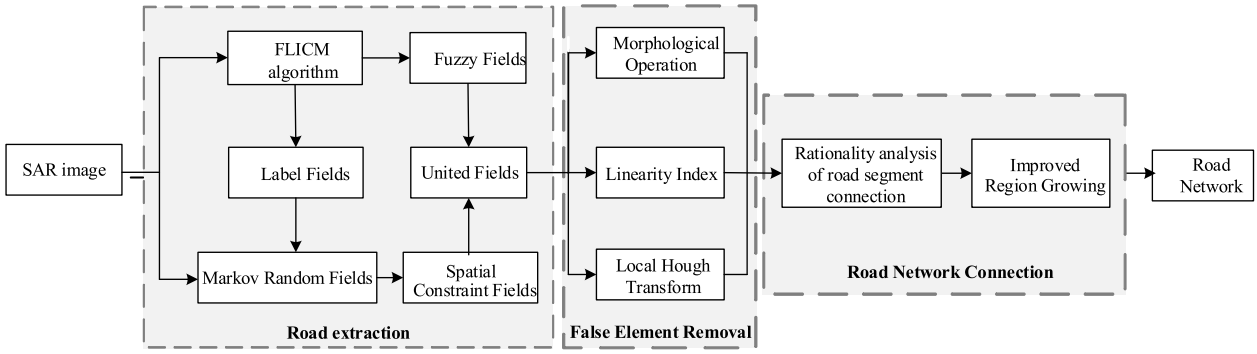

Figure 1 Flowchart of the proposed road network detection

2.1 Road Segment Extraction based on Improved FLICM-MRF Method

The road segment extraction is the first step of road network detection. In this section, an MRF with fuzzy local information C-means clustering (FLICM) based on SAR image GLCM features is proposed. Inspired by the FLICM and MFCM, we incorporate a weighted factor into the objective function, considering the pixel spatial and intensity distances simultaneously.

Since the GLCM has the characteristic of texture feature and the ability to representing the local gray information of an image by statistical method, the GLCM features of an image have been widely used in extraction [9]. GLCM describes the grayscale relationship of statistical space between two nearby points, indicating the frequency of occurrence of a pair of gray levels at a certain position in essence. Because of this aforementioned principle, the grayscale co-occurrence matrix is not sensitive to the periodicity of image texture features and has been proved to be a well-performed method for extracting texture features in SAR images with irregular texture and drastic change.

Haralick et al. proposed 14 kinds of texture feature descriptions based on GLCM [15]. To minimize the complexity of the characteristic matrix information, we test all the 14 GLCM texture feature descriptions firstly. Then, according to the experimental results, the angular second moment, contrast, and entropy can completely describe the texture characteristics of the road in SAR images.

Compared with the traditional hard partition clustering algorithm, the FCM clustering algorithm establishes the degree of uncertainty of samples to categories, which more objectively reflects the physical attribute. The traditional FCM algorithm performs clustering by minimizing the objective formula (1), which is defined as follows.

$$J_m(U,V)=\sum_{k=1}^{n}\sum_{i=1}^{c}u_{ik}^{m}d_{ik}^{2}\left(x_k,v_i\right) \tag{1}$$

where U , V denote the membership degree matrix and the set of clustering center, respectively. Since u_{ik} is the membership degree of the i th element to the class k ,which satisfies $\sum_{i=0}^{c}u_{ik}=1,\forall k=1,\cdots,n$. And $d_{ki}=\left\|x_i-v_k\right\|$, $d_{kj}=\left\|x_j-v_k\right\|$ represent the Euclidean distance.

Although the traditional FCM algorithm has proved to be effective for image segmentation in optical remote sensing, the results in SAR images have underperformed owing to the strong multiplicative speckle noise. Moreover, the FCM algorithm is essentially a local search algorithm based on gradient descent, which is prone to fall into local optimal, and its disadvantages become more obvious as the number of clustering samples increases.

To overcome the above-mentioned disadvantages, an improved FCM named Fuzzy Local Information C-Means (FLICM) clustering method is used in this paper. It can incorporate local spatial and local gray level information in a fuzzy way to preserve robustness and noise insensitiveness, and it is free of any parameter selection. Three selected texture features from GLCM and original gray level information form the input of feature matrix of FLICM, with the spatial attractiveness model between image pixels are fully considered.

$$J\left(U,V\right)=\sum_{k=1}^{n}\sum_{i=1}^{c}\left[\left(u_{ik}\right)^{m}d_{ik}^{2}\left(x_k,v_i\right)+\sum_{j\in N_i}w_{ij}\left(1-u_{kj}\right)^{m}\left(d_{kj}\right)^{2}\right] \tag{2}$$

where, $w_{ij}=1/\left(d_{ij}+1\right)$ is the spatial influence factor; let $W_{ki}=\sum_{j\in N_i}w_{ij}\left(1-u_{kj}\right)^{m}\left(d_{kj}\right)^{2}$ be the spatial influence matrix. And according to the Lagrange multiplier method, necessary conditions for obtaining the minimum value $J\left(U,V\right)$ are:

$$u_{ki}=\frac{1}{\left[\sum_{j=1}^{c}\left(\frac{d_{ki}^{2}+W_{ki}}{d_{ji}^{2}+W_{ki}}\right)\right]^{\frac{2}{m-1}}} \tag{3}$$

$$v_k=\frac{\sum_{k=1}^{n}\left(u_{ik}\right)^{m}x_k}{\sum_{k=1}^{n}\left(u_{ik}\right)^{m}} \tag{4}$$

Markov Random Fields (MRF) algorithm is a typical model-based method, which can effectively describe the prior distribution of the image in terms of the change of image gray level, the arrangement of texture primitively and the internal relation of the local feature information. Specifically, the segmentation method based on MRF can mark the context information of the image and analyze the statistical characteristics of the image. MRF can make use of the correlation between neighborhood pixels to reduce the mutation of pixel values in SAR images. According to the Hammersley-Clifford theorem, MRF can be equivalent to Gibbs distribution.

$$P\left(x\right)=Z^{-1}\exp\left(-U\left(x\right)\right) \tag{5}$$

where $U\left(x\right)=-\beta\sum_{c\in C}V_c\left\{x\right\}$ denotes the energy function, and the value of $V_c\left\{x\right\}$ depends on the local conation of the group C .

$\hat{x}$ is the estimated value of the real label of the segmentation image, and the maximum posterior probability criterion is

$$\hat{x}=\arg\max_{x\in X}\left\{P\left(y\mid x\right)\cdot P\left(x\right)\right\} \tag{6}$$

For SAR images with complex backgrounds, the MRF algorithm can make full use of the spatial relationship information between the image pixel points and adjacent pixels, whose performance in reducing noise is strong. And the

limitation of over-segmentation in the MRF algorithm can be improved by combining the FLICM algorithm, and the joint field is defined as

$$S = \alpha U + (1-\alpha) P \tag{7}$$

where the weight matrix α is used to control the proportion of fuzzy field and spatial constraint field in the extraction procedure. To adjust the proportion automatically, the self-adaptive weight matrix is proposed as follows:

$$\alpha_k = \begin{cases} \dfrac{\sum_{j \in N_i} w_{ij} r_{ij}}{\sum_{j \in N_i} w_{ij}}, \left| x_k - \bar{m} \right| \le \dfrac{\sigma_j}{2} \\ 0 \qquad , \left| x_k - \bar{m} \right| > \dfrac{\sigma_j}{2} \end{cases} \tag{8}$$

$$r_{ij} = \frac{\left| x_{ij} - \bar{m} \right|}{\sigma_j + \left| x_{ij} - \bar{m} \right| + 1} \tag{9}$$

x_k is a pixel in the de-noised image, who belonging to the neighborhood pixel system N_i, that is, $x_k \in N_i$. σ_i and $\bar{m}$ represents the variance and mean in the neighborhood pixel system N_i. If the value of distance $\left| x_k - \bar{m} \right|$ is larger than $\frac{\sigma_i}{2}$, it demonstrates this point is isolated noise point and let α_k be 0. On the contrary, it is judged to be an inner point, and the weight valve is determined by the spatial gray level fluctuation condition in the neighborhood: r_{ij} denotes the relationship between variance and mean in the neighborhood pixels, which can be used to be a parameter reflecting the gray level fluctuation of the image. The spatial correlation of image pixels reflects the degree of spatial attraction so that we utilize $w_{ij} r_{ij}$ to show the condition of spatial gray level fluctuation under different spatial attractions. Therefore, the weight of the fuzzy field combined with the constraint field can be obtained adaptively by using the proposed parameter.

2.2 False Road Element Removal Processing

The extracted road elements obtained from the previous section, containing the relatively complete fragments, broken segment and the false extracted road elements. To discard false-alarm elements, this section utilizes the combination of the local operations to remove false road segment candidates and normalize the overall direction of line primitives by extracting the centerline.

Compared with other land targets, roads have obvious geometric linear features. First, the same-regional roads have similar intensity and width. Then, the direction of the road changes slowly, which means length-width ratio of roads are larger than nearby ground objects. Finally, according to the functional properties of the road, roads are not cut off for no reason and the length or width of any road are limited in SAR images.

The results are processed by mathematical morphology to disconnect the adhesion between the road elements and false road elements. By calculating the linearity characteristics of the candidate road areas, some nonlinear targets (such as buildings, grasslands, etc.) can be effectively eliminated. A new rectangle is defined by counting the area of the region and the diagonal length of its minimum enclosing rectangle. The ratio is defined as followed.

$$LFI = \frac{L}{W} = \frac{L}{s_i / L} = \frac{L^2}{s_i} \tag{10}$$

where L, W denote the length and width of the new rectangle, and s_i is the area of each connected region.

In general, the curvature of a road is typically slight, so in the local region, most parts of the roads can be considered as straight lines. Therefore, the image after LFI is divided into several sub-images, and local Hough transform is adopted to extract line primitives that meet the restricted conditions. The missed area is easily formed between the gap of two sub-images, as a result, there should be partly overlapped in the sub-images. Then, the results are combined to obtain the centerline of the whole image by LSD algorithm.

2.3 Road Network Connection

The detection image after the centerline procedure has the following characteristics: 1) small amount of short line elements remain; 2) part of the extracted road line primitives are non-road areas or some road segment are positionally

shifted slightly;3) due to the image quality and the shadow of the surrounding objects, some of the continuous road elements are not extracted successfully.

What can we see is that the detected line primitives do not form a complete road network so that the lines need to be reconstructed together. The traditional RG algorithm directly utilizes the grayscale region membership criteria of a single endpoint of the road line element and the pixels around the seed region. Because of the effect of speckle noise on SAR images, it is meaningless to judge the criteria on the basis of a single pixel. Furthermore, when the distance between the endpoints is shorter than some threshold, it can be put into the seed region without considering the constraints are unreasonable, which will cause illogical connection and the increase of computational amount and complexity.

To guarantee computation efficiency and enhance accuracy, an improved RG algorithm with the rationality of connection analysis for road network reconstruction is proposed. A more reasonable constraint takes into full account the approximate parallel and vertical spatial geometry between adjacent line primitives of the road centerlines, and the endpoints which satisfy reasonable constraints form the initial seed points to be grown in the improved RG algorithm.

2.3.1 Rationality of Road Segment Connection

In case of the distance between the endpoints and general direction information of the road elements are not considered, the reconstruction constraint conditions can be unreasonable and will greatly increase the computational amount and complexity of the subsequent road network connection, as shown in Figure 2(a). In this paper, the spatial geometric relationship between adjacent road elements is fully considered, and constraints for reasonable road network connection are considered from four aspects as a whole, as shown in Figure 2(b).

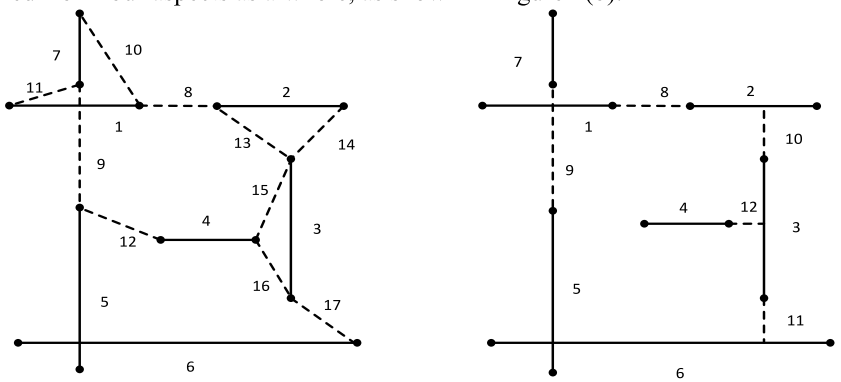

(a) (b)

Figure 2 Road network detection rationalization connection comparison (a) Unreasonable road segment connection, (b) Reasonable road segment connection

The rationality analysis of road network connection is beneficial to determine whether the point in the search region is the waiting connected fragment or the information of road termination, and it is composed of the following four aspects: distance, proximity, directionality, and overlap.

Distance between the endpoints of the nearby road fragments is one of the most important parameters reflecting the degree of credibility of reconstruction. The distance l_{ij} indicates the spatial position relation of road elements that the less likely two elements belonging to the same original road when the distance is longer.

$$D_{ij} = \frac{1}{l_{ij}+1} \tag{11}$$

The length of two fragments is r_i and r_j, respectively, and the sum of the length of those segment region is $Len = r_i + r_j + l_{ij}$. Then, the proximity function of line primitives P_{ij} is defined as:

$$P_{ij} = \frac{r_i + r_j}{Len} \tag{12}$$

Considering that the direction of road element exists in two states, nearly parallel and nearly perpendicular, then the directionality S_{ij} is defined as follows:

$$\begin{cases} S_{ij} = \dfrac{1}{\sin\left|\theta_i - \theta_j\right| + 1} & if \text{ parallel} \\ S_{ij} = \dfrac{1}{\cos\left|\theta_i - \theta_j\right| + 1} & else \end{cases} \tag{13}$$

where the direction of road line is θ_i and θ_j, separately.

Since p_{i1} and q_{j1} are corresponding endpoints of two road linear primitives and the vertical projection distance d_{ij} from q_{j1} to the road element i demonstrates the degree of overlap, and probability function Q_{ij} can be set as:

$$Q_{ij} = 1 - \frac{d_{ij}}{Len} \tag{14}$$

The establishment of the spatial and geometric constraint function M_{ij} based on the above four aspects measures the possibility of a reasonable connection between the road segment endpoints, which means if it is larger than the threshold value, it is judged to be part of the road network fragment.

$$M_{ij} = \max\left(\alpha D_{ij} + \beta P_{ij} + \gamma S_{ij} + \sigma Q_{ij}\right) \tag{15}$$

whereas α、β、γ and σ are the proportionality coefficients, which are set as 0.5 in this paper.

2.3.2 Reconstruction of Road Network based on Improved Region Growing

According to the rationality of road network processing, the initial seed endpoints which satisfy reasonable constraints are obtained. When using the traditional RG algorithm which does not consider the particularity of SAR image, it will cause the following problems: firstly, due to the influence of speckle noise, it is meaningless to use the gray value of a single pixel as the judgment standard of gray threshold in SAR images; Secondly, as the growth path of traditional RG method is based on the limited surrounding pixels, it leads to a large amount of overall computation and data storage.

Therefore, this paper proposes a road network reconstruction method based on the improved RG algorithm for SAR images. First of all, the average gray value I_m of the seed road areas in original SAR image is calculated according to different connected domains, which is used as the gray characteristic standard for the growth. Then, to reduce the effect of solitary point noise, the local search area is divided into several different direction strips, whose average gray value and direction are calculated, and if the strip meets the criteria, it is merged into the seed region. Finally, the seed road segment is divided into some sub-fragments, and eight direction detectors are used respectively to obtain the maximum response direction information. All the maximum responses are integrated to acquire the average direction of the seed road element, which is named the seed direction θ_l.

The restrictions on the search region are defined as follows to guarantee accuracy and computational efficiency. Firstly, on the basis of radiation characteristic of SAR image, it can be seen that roads have internal scattering uniformity and the overall variance of the gray level is small, that is, if the difference between the gray level mean of the region to be grown and the statistical gray level mean of seed road element I_m is less than the preset threshold, the gray level growth condition is satisfied. Secondly, because the direction of the seed road changes slowly which means curvature is basically constant, the angle range of the search region should be within the $\pm\theta_{\max}$ centered on the average direction θ_l of seed road element. Lastly, as for the search step size, the search range is 1 to $r_{\max}$ with its sampling interval is 1 pixel unit.

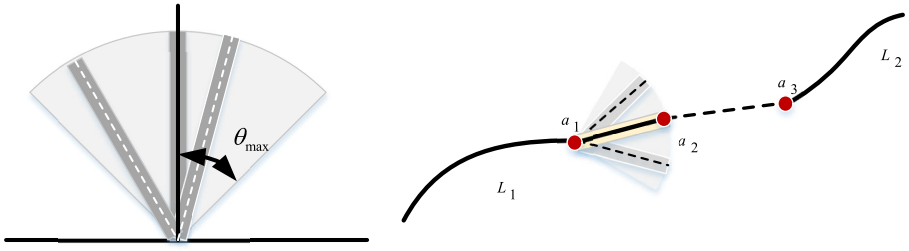

Figure 3 Improved region growth algorithm

As is shown in Figure 3, set road element L_1 as the seed with endpoint a_1 is initial grow point, taking the maximum

search radius $r_{\max}$ within 1° sampling interval to estimate the criteria of grayscale and direction as shown in equation (22) in the restricted search area. After traversing the entire search region, the optimal strip $\left(\hat{r},\Delta\hat{\theta}\right)$ is compared with the preset threshold value R_{th}, and when it is lower than the threshold value, it is taken as the candidate growing area under this point seed and a_2 is taken as the next initial point used for the next search round. If there is no strip satisfies the region membership criteria, the road seed stops growing.

The selection criteria of the optimal strip for each growth are determined by the following formula:

$$\left(\hat{r},\Delta\hat{\theta}\right)=\min_{r\in[r_{\min},r_{\max}],\Delta\theta\in[-\Delta\theta_{\max},\Delta\theta_{\max}]}\left(f\left(r,\Delta\theta\right)\right) \tag{16}$$

$$f\left(r,\Delta\theta\right)=\alpha\cdot\frac{2}{1+e^{-0.5\Delta\theta}}+\beta\cdot\frac{s^2}{g+a} \tag{17}$$

where,

$$\left.\begin{aligned} g&=\frac{1}{r}\sum_{t=1}^{r}abs\left(I'\left(x_{r\theta},\mathrm{y}_{r\theta}\right)-I_m\right)\\ \Delta\theta&=\frac{1}{r}\sum_{t=1}^{r}abs\left(angle\left(x_{r\theta},\mathrm{y}_{r\theta}\right)-\theta_l\right)\\ I'\left(x_{r\theta},\mathrm{y}_{r\theta}\right)&=\frac{1}{9}\sum_{m=-1}^{1}\sum_{n=-1}^{1}I\left(x_{r\theta}+m,\mathrm{y}_{r\theta}+n\right)\end{aligned}\right\} \tag{18}$$

where α, β denote scale factor which set as $\alpha=0.5$, $\beta=0.5$ in this paper; the additional weight value a set to prevent the gray difference from being too small; and s is the shape scale factor of the strip area to be grown.

3. EXPERIMENT AND DISCUSSION

To verify the performance of the proposed method, two data sets from GF-3 SAR satellite have been used in this paper, including a suburban region in Shanghai(China) acquired by GF-3 sensor with the spatial resolution of 5.29m, and an urban area in Qingdao(China) obtained by GF-3 sensor with the spatial resolution of 2.57m. Figure 4 shows the original SAR images respectively.

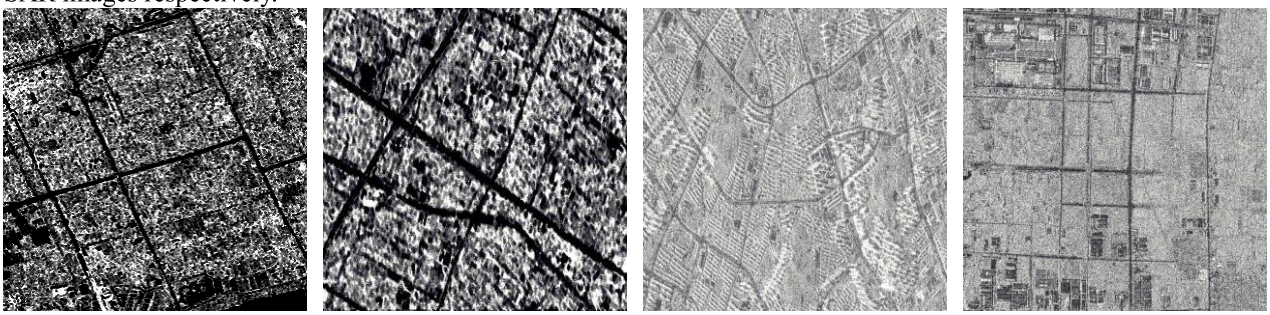

(a) (b) (c) (d)

Figure 4 SAR amplitude of four experimental test areas (a) area 1 (b) area 2 (c) area 3 (d) area4

Figure 5 shows the results of the road element extraction using the FLICM clustering method, FCM_S algorithm and the proposed method, respectively. The result extracted by the FCM_S algorithm is shown in Figure 5(b), comparing with the method proposed in this paper, restrains a lot of speckle to some extent, while some image details are lost and the overall extraction is not very accurate. In Figure 5(c), FLICM algorithm can get relatively good results due to the consideration of the spatial correlation between pixels, however, there are still many false extracted elements near the extracted candidate road edge. Among the above-mentioned algorithms, the proposed method [Figure 5(d)] in this paper obtains the best extraction result by visual inspection, which means that it is most robust to speckle noise and can maintain more details.

(a) (b) (c) (d)

Figure 5 Comparison of road extraction results (a) original SAR image. (b) road extraction result of FCM_S. (c) road extraction result of FLICM. (d) road extraction result of the proposed method.

To effectively facilitate the evaluation of the detection of the road network, Figure 6(a) respectively shows the ground truth of the testing region, and the road network reconstruction results connected by utilizing the improved region growth algorithm proposed in this paper of four experimental data as shown in Figure 6(b). Furthermore, by means of contrasting the proposed algorithm with the method in [16], which are shown in Figure 6(c). While the white line means correct detected road element; the yellow lines are undetected road parts, and; the red lines are false detected fragments. The circled areas are the differences between the two algorithms.

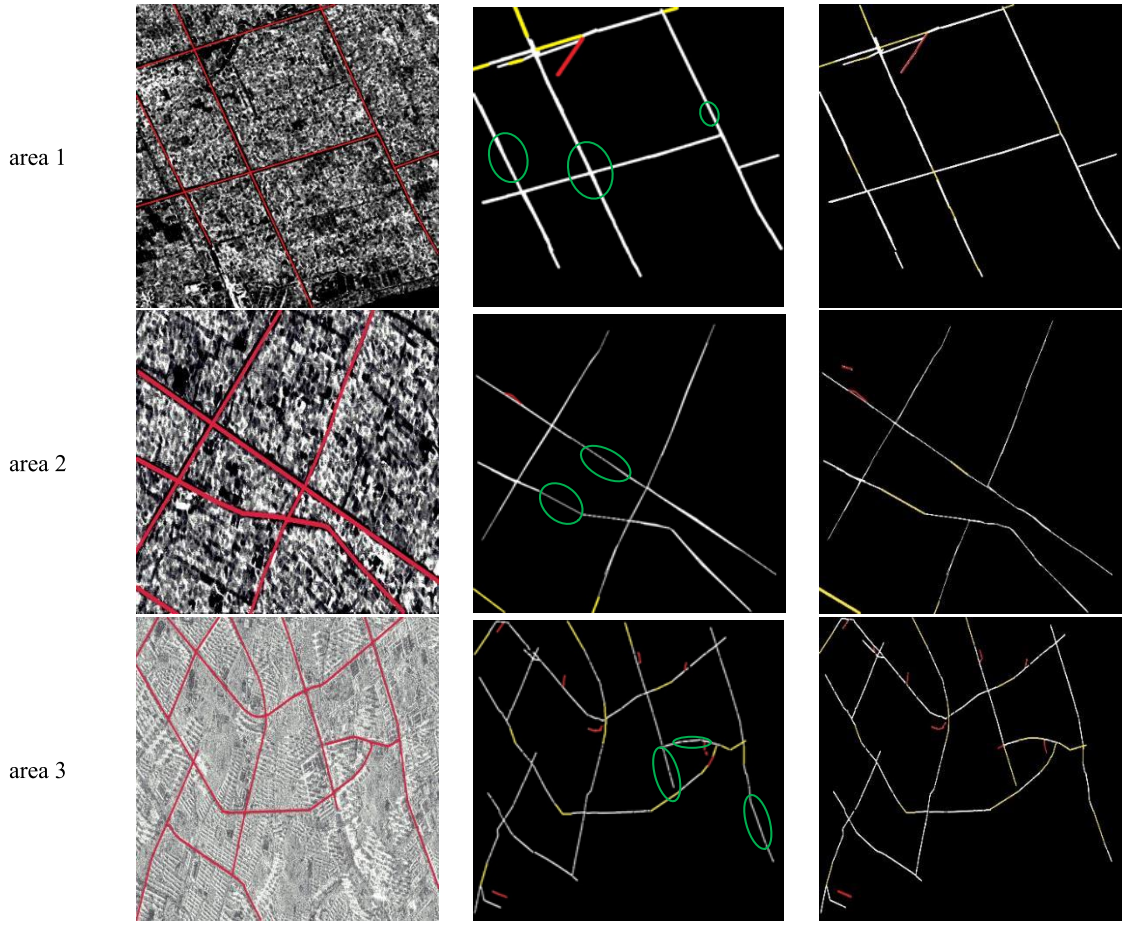

area 4

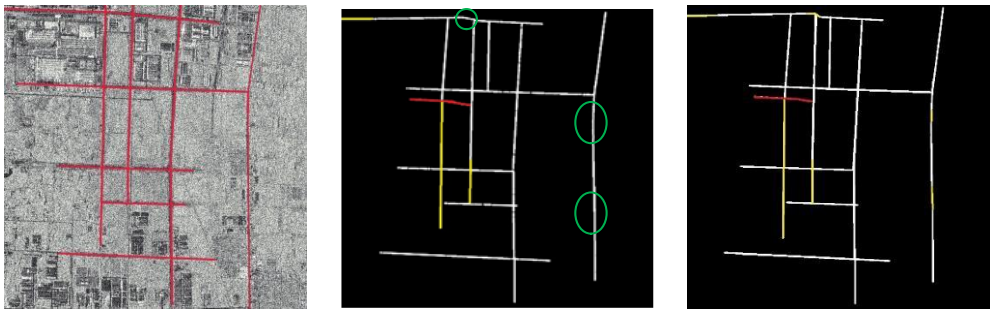

(a) (b) (c)

Figure 6 Comparison of road network detection results (a) ground truth. (b) the proposed method. (c) the method in reference [16].

Table 1 lists the calculation time between algorithms of road network detection. The tests in this paper is under the hardware condition of 2.4GHz main frequency central processing unit (CPU) and 8-GB RAM memory, and the primary programing language used as the program implementation is Visual Studio 2012. The second column shows the size of the four images. The third column shows the computation time for road elements extraction using the FLICM method, and the computation time of the proposed method is shown in the fourth column. The fifth column lists the computation time of the RG algorithm proposed in [16]. The sixth column lists the computation time of the improved RG algorithm. From Table 1, we can see the total time mainly depends on the sizes of the images and the amounts of the contained roads. The computational efficiency is about the same between the FLICM and the proposed method in these four images, and the computational time of the improved RG algorithm proposed in this paper is slightly shorter than that of the traditional RG algorithm.

Table 1 Computation time of different algorithms

image	size	FLICM	FLICM_MRF	RG	improved RG
a	998*1000	360s	372.s	20s	18s
b	1206*533	241s	274s	15s	13s
c	1553*1083	451s	548s	24s	22s
d	1169*1249	392s	426s	17s	12s

Then, three indicators include road detection integrity rate, accuracy rate, and quality factor were selected for performance evaluation, with the results in [16] were compared and analyzed. According to Figure7 and Table 2, intuitive and quantitative comparison results are presented respectively. In terms of road detection accuracy, both methods can get a relatively high accuracy rate. However, the road integrity rate and quality factor proposed in this paper are obviously superior to the above-mentioned method, especially for the relatively complex road network in the image.

Table 2 Evaluation index of road network detection results

image	The proposed method			The method in[16]		
	integrity	accuracy	quality factor	integrity	accuracy	quality factor
a	97.06%	95.12%	92.44%	95.28%	95.04%	90.77%
b	96.15%	94.37%	90.94%	92.38%	93.75%	87.01%
c	75.56%	90.48%	70.06%	73.85%	88.89%	67.61%
d	81.19%	96.92%	80.15%	78.16%	96.77%	76.17%

4. CONCLUSION

High-resolution SAR images are rich in details and have numerous ground objects, while at the same time, it means more complex background interferences near the road elements. To solve the above mentioned problems, this paper proposes a new three-step road network detection method for High-resolution SAR images. Firstly, a new method for extracting the road candidate elements named FLICM-MRF algorithm is proposed, which is significantly improve the overall quality of road extraction processing. Secondly, an improved RG algorithm for road network connections for SAR images is proposed. And according to the experimental results, the reconstruction for the fractured part of the road is more reasonable and accurate.

REFERENCE

[1] Chen, Q., et al. "Unsupervised Land Cover/Land Use Classification Using PolSAR Imagery Based on Scattering Similarity." *Geoscience & Remote Sensing IEEE Transactions* on 51(3):p.1817-1825(2013).

[2] Li, Wenmei, et al. "Forest aboveground biomass estimation using polarization coherence tomography and PolSAR segmentation." *International Journal of Remote Sensing* 36.2:530-550(2015).

[3] S. Chen, H. Ma, Y. Fan, F. Xu, and J. Lian, "Road damage assessment from high resolution satellite remote sensing imagery in Wenchuan Earthquake," *J. Remote Sens.*, vol. 6, pp. 6–17(2008).

[4] Fjortoft, et al. "An optimal multiedge detector for SAR image segmentation. " *IEEE Transactions on Geoscience & Remote Sensing* ,vol. 36, no. 3, pp. 793–802 (1998).

[5] Tupin, et al. "Detection of linear features in SAR images: application to road network extraction." *Geoscience and Remote Sensing, IEEE Transactions* on vol. 36, no. 2, pp. 434–453(1998).

[6] C. Lemarechal, R. Fjortoft, et al. "SAR image segmentation by morphological methods." *Proceedings of SPIE - The International Society for Optical Engineering* 3497:111-121(1998).

[7] Krinidis, Stelios, and V. Chatzis . "A Robust Fuzzy Local Information C-Means Clustering Algorithm." *IEEE Transactions on Image Processing* 19(5):1328-1337(2010).

[8] Q. Miao, R. Liu, et al. "A Semi-supervised Image Classification Model based on Improved Ensemble Projection Algorithm." *IEEE Access* 6:1372-1379(2018).

[9] F. Xiao and L. Tong . "A Road Extraction Method Using Dual-Temporal High-Resolution SAR Images." *IGARSS 2019 - 2019 IEEE International Geoscience and Remote Sensing Symposium IEEE*, pp. 1216-1219(2019).

[10] J. B. Burns, et al. "Extracting Straight Lines." *Pattern Analysis and Machine Intelligence, IEEE Transactions* on vol. PAMI-8, no. 4, pp. 425-455(1986).

[11] Kang, Chee Woo, R. H. Park , and K. H. Lee . "Extraction of straight line segments using rotation transformation: generalized hough transformation." *Pattern Recognition* 24(7):633-641(1991).

[12] Byoung-Ki Jeon, Jeong-Hun Jang and Ki-Sang Hong, "Road detection in spaceborne SAR images using a genetic algorithm," *IEEE Transactions on Geoscience and Remote Sensing*, vol. 40, no. 1, pp. 22-29(2002).

[13] Negri, M., et al. "Junction-aware extraction and regularization of urban road networks in high-resolution SAR images." *IEEE Transactions on Geoscience & Remote Sensing* 44(10):2962-2971(2006).

[14] Tupin, et al. "Road detection in dense urban areas using SAR imagery and the usefulness of multiple views," *IEEE Transactions on Geoscience & Remote Sensing* 40(11): 2405-2414 (2002).

[15] P. Lu, K. Du, et al. "A New Region Growing-Based Method for Road Network Extraction and Its Application on Different Resolution SAR Images." *IEEE Journal of Selected Topics in Applied Earth Observations & Remote Sensing* 7(12):4772-4783(2015).

[16] T. Zeng, Q. Gao, et al. "Road Network Extraction From Low-Contrast SAR Images." *IEEE Geoscience and Remote Sensing Letters* 16(6):907-911(2019).